

# Highly Sensitive Detection of Organophosphorus Pesticides Represented by Methamidophos via Inner Filter Effect of Au Nanoparticles on the Fluorescence of CdTe Quantum Dots

Jiajia Guo · Hongkun Li · Meng Xue · Minwei Zhang ·  
Xianyi Cao · Yeli Luo · Fei Shen · Chunyan Sun

Received: 14 June 2013 / Accepted: 8 October 2013 / Published online: 23 October 2013  
© Springer Science+Business Media New York 2013

**Abstract** A sensitive fluorescence detection method of organophosphate pesticides (OPs) represented by methamidophos was developed using the inner filter effect (IFE) of Au nanoparticles (AuNPs) on CdTe quantum dots (QDs). The fluorescence of CdTe QDs was remarkably quenched with the presence of AuNPs via IFE. Acetylcholinesterase (AChE) catalyzed the hydrolysis of acetylthiocholine into thiocholine, which could induce the aggregation of AuNPs and decrease their characteristic absorption, making IFE-decreased fluorescence of CdTe QDs recovered. OPs can inhibit the activity of AChE, thus preventing the aggregation of AuNPs and the fluorescence recovery of CdTe QDs. Therefore, the IFE of fluorescence between AuNPs and CdTe QDs could convert the absorption signal to fluorescence signal, which improved the detection sensitivity of OPs in vegetables. Under the optimum conditions, the response was linearly proportional to the concentration of methamidophos in the range of 0.06–0.78 mg/kg with a detection limit of 2 µg/kg ( $3\sigma$ ) which was superior to the method of GB/T 5009.199-2003. The proposed assay exhibited good reproducibility and accuracy, providing a simple and rapid method for the screening of OPs.

**Keywords** Inner filter effect · Quantum dots · Au nanoparticles · Fluorescence · Methamidophos

J. Guo · H. Li · M. Xue · M. Zhang · X. Cao · Y. Luo · F. Shen ·  
C. Sun (✉)  
Department of Food Quality and Safety, Jilin University,  
Changchun 130062, China  
e-mail: sunchuny@jlu.edu.cn

C. Sun  
e-mail: sunchunyan1977@163.com

## Introduction

Organophosphates (OPs) are widely used as pesticides in modern agriculture due to their high insecticidal activity and relatively low persistence. Unfortunately, these compounds exhibit high acute toxicity, with the majority being hazardous to both human health and the environment. Indeed, the inhibition of acetylcholinesterase (AChE) activity by OPs can lead to a disturbance of normal neuronal function and even death (Xue et al. 2012; Chauhan and Pundir 2012). The standard reference methods for the determination of pesticide residues in real samples are mainly based on gas chromatography (Chai and Tan 2009; Qu et al. 2010) or high-performance liquid chromatography (HPLC) (Perez-Ruiz et al. 2005; Sanz et al. 2004). These two traditional methods have the same disadvantages, such as time-consuming procedures, complicated operations, and high-cost expenses. Hence, it is necessary to develop the simple, rapid, and low-cost methods for determination of pesticide residues.

Recently, considerable efforts have been devoted to develop nanosensors for OPs because they can provide rapid, sensitive, simple, low-cost, and on-site detection by cooperative recognition and signaling (Liu et al. 2008; Periasamy et al. 2009). These nanosensors are mainly based on the inhibition effects of OPs on catalytic activity of AChE for the hydrolysis reaction of acetylcholine to choline. On the other hand, various configurations and transduction techniques using nanomaterials for the optical/electronic sensing of OPs have been explored. For example, Au nanoparticles (AuNPs)-based colorimetric assays have recently become useful for many types of analytes without the need for advanced instruments because molecular recognition events can be transformed into color changes, which are highly sensitive to the size, shape, capping agents,

and medium refractive index, as well as the aggregation states of AuNPs (Liu et al. 2012; Zhao et al. 2008; Wang and Guo 2009). Quantum dots (QDs) are inorganic fluorophores with unique optical and electronic properties, which have attracted great research interest in the past two decades in various fields such as imaging, biolabeling, and chemical and biological assay (Byers and Hitchman 2011; Gill et al. 2008; Frasco and Chaniotakis 2009). The photoluminescent CdS QDs have been used as probes for detection of OPs in an AChE/acetylthiocholine enzyme catalytic reaction system (Yu et al. 2009). Based on the fluorescence switch of QDs, Liu et al. prepared a biosensor for the detection of OPs in real fruit and vegetable samples, which was fabricated using the layer-by-layer assembly technique (Zheng et al. 2011). Meng et al. (2013) developed a simple and sensitive fluorescence biosensor for detection of OPs using H<sub>2</sub>O<sub>2</sub>-sensitive QDs and AChE/choline oxidase bi-enzyme. Herein, we report a highly sensitive optical biosensor for the detection of OPs represented by methamidophos in vegetables based on the inner filter effect (IFE) of AuNPs on the fluorescence of CdTe QDs.

The mechanism of IFE refers to the absorption of the excitation and/or emission light of fluorophores by absorbers (quenchers) in the detection system (Yuan and Walt 1987). The IFE is a source of errors in fluorometry, but it can be applied to develop novel optical assays by converting the absorption signals into fluorescence signals (Shao et al. 2005; Wang et al. 2011). Since the changes in the absorbance of the absorber translate into exponential changes in the fluorescence of the fluorophore, an enhanced sensitivity for the analytical method is reasonable with respect to the absorbance alone (Shao et al. 2005). Moreover, these sensors do not require the establishment of any covalent linking between the absorber and fluorophore but utilize them as such. However, the limited choice of suitable absorber and fluorophore restricts the application of IFE-based fluorescence assay because IFE would occur effectively only if the absorption band of the absorber possesses a complementary overlap with the excitation or emission bands of the fluorophore. AuNPs have tremendously larger extinction coefficient (about 10<sup>8</sup> M<sup>-1</sup> cm<sup>-1</sup> or more) than the conventional chromophores, which enables AuNPs as extraordinarily effective absorbers in IFE-based fluorescence assay (Shang and Dong 2009). On the other hand, QDs can perform the role of potentially ideal fluorophore due to their superior optical properties such as high quantum yield of fluorescence, narrow/symmetric emission spectrum, and size- and composition-tunable emission wavelength (Xu et al. 2011).

The principle of the proposed IFE-based assay for OPs is illustrated in Scheme 1 by using AuNPs and QDs as the partner of absorber/fluorophore. The as-prepared citrate-stabilized AuNPs are claret red and well dispersed. Due to

the strong absorption of AuNPs at 522 nm, the fluorescence of thioglycolic acid-capped CdTe QDs is obviously quenched in the presence of citrate-stabilized AuNPs via IFE (1). Positively charged acetylthiocholine is employed as the substrate for AChE and is inclined to adsorb onto the surface of negatively charged AuNPs via electrostatic interactions. AChE catalyzes the hydrolysis of acetylthiocholine to produce thiocholine, which is positively charged and bears an additional thiol group (–SH). Due to this characteristic, thiocholine can substitute the citrate and easily bind onto the surfaces of AuNPs. As a result, crosslinking and aggregation of AuNPs would occur due to the electrostatic interactions and the strong Au–SH interaction, leading to the decrease of absorbance of AuNPs. As a result, the IFE-decreased emission of CdTe QDs is restored. The presence of OPs can irreversibly inhibit the catalytic activity of AChE and the aggregation of AuNPs, and the emission is decreased again at a certain degree (2). Thus, the fluorescence emission of CdTe QDs could be modulated by the absorption of AuNPs which varies with the concentration of OPs, making the fluorescence analysis of pesticides feasible. Our results demonstrate that the proposed IFE-based optical biosensor could be successfully applied to determine low concentrations of OPs in real vegetable samples.

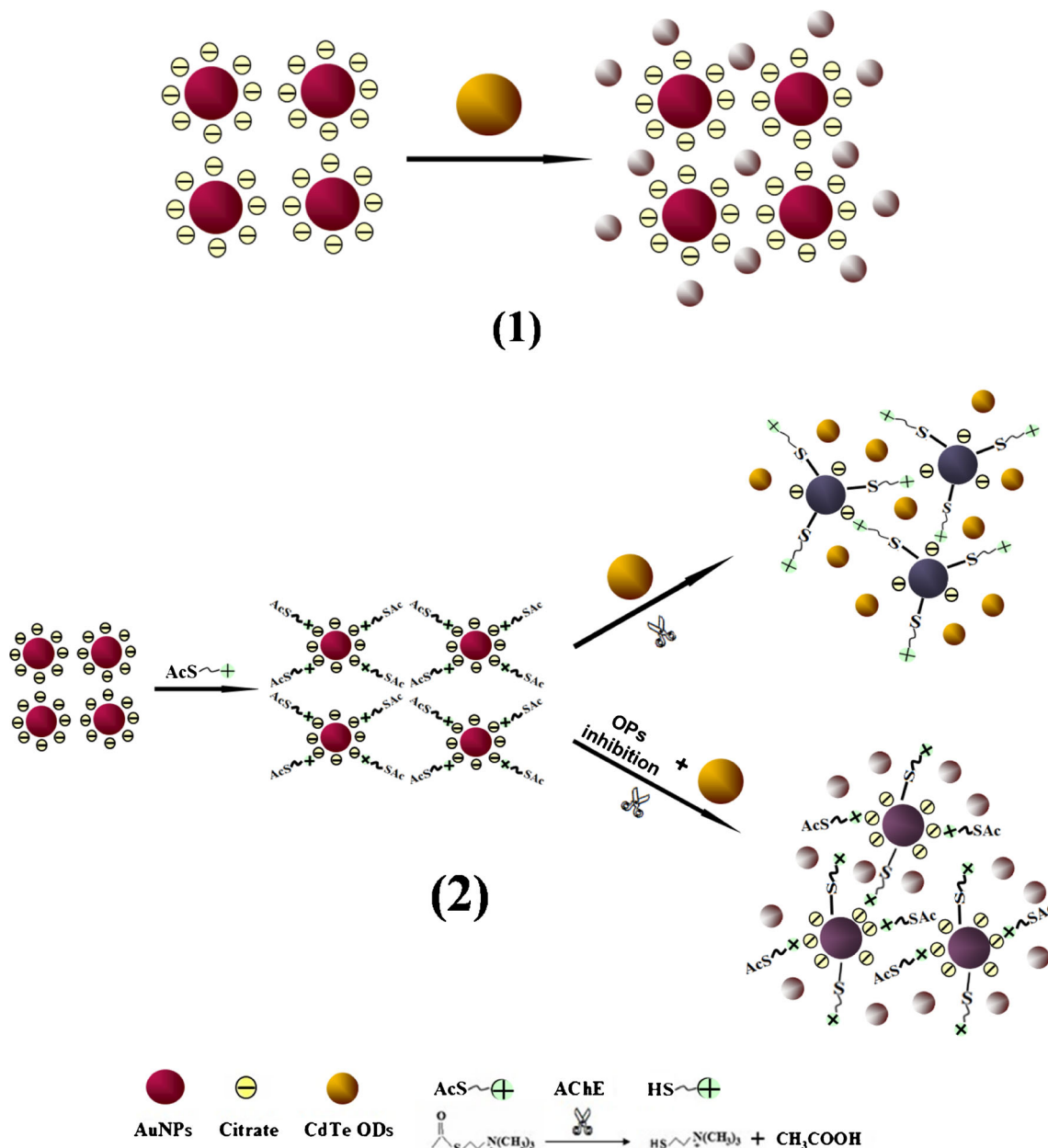
## Experimental

### Reagents and Materials

Acetylthiocholine iodide (ATI), acetylcholinesterase (AChE, type C3389, 500 U mg<sup>-1</sup> from electric eel), and methamidophos were purchased from Sigma-Aldrich (St. Louis, USA). Te powder, sodium borohydride (NaBH<sub>4</sub>), and thioglycolic acid (TGA) were obtained from Sinopharm Chemical Reagent (Shanghai, China). Cadmium chloride (CdCl<sub>2</sub>·2H<sub>2</sub>O), AuCl<sub>3</sub>·HCl·4H<sub>2</sub>O, sodium citrate, vitamin C, vitamin B<sub>1</sub>, vitamin B<sub>2</sub>, FeCl<sub>3</sub>, NaCl, MgCl<sub>2</sub>, ZnCl<sub>2</sub>, and KCl were purchased from Beijing Chemical Reagent Company (Beijing, China). Methanol (HPLC grade) was purchased from Fisher Scientific (USA). If not specifically stated, all the chemicals were of analytical grade and triply distilled water was used in all experiments. Organic vegetable free from pesticides was purchased from the local supermarket.

### Apparatus

The fluorescence spectra were acquired on a RF-5301 fluorescence spectrophotometer (Shimadzu, Tokyo, Japan) at the excitation wavelength of 400 nm, with both of the exciting and emission slits set at 5 nm. UV–vis absorption spectra were recorded with a 2550 UV–vis spectrophotometer (Shimadzu, Tokyo, Japan). Zeta potential ( $\zeta$ ) was performed on a Zeta



**Scheme 1** Schematic illustration of rapid analysis of OPs based on enzyme inhibition using inner filter effect of AuNPs on the fluorescence of CdTe QDs

Sizer Nano ZS particle analyzer. A WVFY-201 microwave reactor of 800 W power (Zhize Equipment Factory, Shanghai, China) was used in the experiments. Transmission electron microscopy (TEM) measurements were made on a TECNAI F20 (FEI Co., Holland) operated at an accelerating voltage of 200 kV. The samples for TEM characterization were prepared by placing a drop of colloidal solution on carbon-coated copper grid and dried at room temperature. All pH measurements were carried out with a Model pHs-3C (Chenghua Equipment Factory, Shanghai, China). The centrifugation was performed on a CR20B2 refrigerated centrifuge (Tokyo, Japan). The ultrasonic treatment was

carried out on a 125 KQ-300DE ultrasonicator (Kunshan Ultrasonic Instrument Co., Shanghai, China).

#### Synthesis, Purification, and Characterization of Water-Soluble TGA–CdTe QDs

TGA-capped CdTe QDs were synthesized according to the procedure described in the reference (Zhang et al. 2012). Briefly, 0.0256 g Te powder and 0.0386 g NaBH<sub>4</sub> were firstly added into 1 mL water in a three-neck flask with a condenser attached and reacted at 50 °C for 45 min to get Te precursor (NaHTe). Cd precursor was prepared by mixing a solution of

CdCl<sub>2</sub> (0.09134 g) with 66 μL TGA, and the solution was diluted to 100 mL, which was then adjusted to pH 11 by 1 M NaOH and deaerated with N<sub>2</sub> for 20 min. The Cd precursor was added into NaHTe solution while stirring vigorously at room temperature. The molar ratio of Cd<sup>2+</sup>/Te<sup>2-</sup>/TGA is 1:0.5:2.4. Under the protection of N<sub>2</sub> atmosphere, the mixed solution was stirred for 10 min and then heated with microwaves at 50 % output power for 45 min. The crude CdTe QDs solution was washed with equal isopropanol and centrifuged to remove excess precursors. Then, the QDs deposit was dried by vacuum desiccation. Finally, the prepared TGA–CdTe QDs were dispersed in water. According to the calculation method mentioned in a previous literature (Yu et al. 2003), the particle size of the as-prepared TGA–CdTe QDs was 2.3 nm and the molar concentration of CdTe QDs was calculated to be approximately  $1.24 \times 10^{-5}$  mol L<sup>-1</sup>.

#### Preparation of Citrate-Stabilized AuNPs

The colloidal solution of 13 nm citrate-stabilized AuNPs was prepared according to the reference (Li et al. 2011) and stored at 4 °C. All glassware used in these preparations was thoroughly cleaned in aqua regia, rinsed with triply distilled water, and oven-dried prior to use. In a 250-mL round-bottom flask equipped with a condenser, 100 mL of 1 mM HAuCl<sub>4</sub> was heated to a rolling boil with vigorous stirring. Rapid addition of 10 mL of 38.8 mM sodium citrate to the vortex of the solution resulted in a color change from pale yellow to claret red. Boiling was continued for 10 min; the heating mantle was then removed, and stirring was continued for an additional 15 min. After the solution cooled down to room temperature, it was filtered through a 0.4-μm Millipore membrane filter. The molar extinction coefficient at ~520 nm for 13 nm spherical AuNPs is  $2.7 \times 10^8$  M<sup>-1</sup> cm<sup>-1</sup> (Zhao et al. 2008); thus, the molar concentration of AuNPs was calculated to be approximately  $3.7 \times 10^{-9}$  mol L<sup>-1</sup> according to the Lambert Beer's law.

#### General Procedures for Fluorescence Titration of Methamidophos

A typical IFE analysis of methamidophos was performed as follows. 1 mL AuNPs ( $1.85 \times 10^{-9}$  mol L<sup>-1</sup>) and 0.2 mL ATI (10 μmol L<sup>-1</sup>) were added into 5-mL centrifuge tubes with 0.5 mL different concentrations of methamidophos, followed by addition of 20 μL AChE (1,000 mU mL<sup>-1</sup>). And then 1 mL CdTe QDs ( $1.24 \times 10^{-6}$  mol L<sup>-1</sup>) was added into the system. The fluorescence spectra of the reacted solutions were recorded, and the calibration curve for methamidophos was established according to the  $(F_0 - F)/F_0$  where  $F$  and  $F_0$  are the maximum emission intensity of the system in the presence and absence of pesticide, respectively. Each experiment was replicated three times, and the average was used for analysis.

#### Procedures for Methamidophos Sensing in Spiked and Real Vegetable Samples

Methamidophos in Chinese cabbage was measured to evaluate the potential of this assay for pesticides screening in real-world applications. The vegetable samples were pretreated according to the reference (Pérez-Ruiz et al. 2001). Ten grams of vegetable samples was weighed and finely chopped and then dissolved in 50 mL methanol and ultrasonicated for 60 min. The sample mixture was centrifuged, and the supernatant was further filtered. The filtrate was concentrated to almost dry at 50 °C by a vacuum rotary evaporator. The residue was diluted with water to 5 mL for detection according to the method in “General Procedures for Fluorescence Titration of Methamidophos.” A certain amount of methamidophos was added into the vegetable samples and then pretreated and analyzed in accordance with the above procedure.

The accuracy of the proposed rapid fluorescent biosensor for OPs detection in real contaminated vegetable sample was compared with enzyme inhibition rate method of Chinese National Standards (2003) GB/T 5009.199-2003. The standard detection method in GB/T5009.199-2003 is based on the principle that the hydrolyzate of acetylcholine catalyzed by AChE reacts with DTNB, forming a yellow substance with the maximum absorbance at 412 nm, whereas the presence of OPs can irreversibly inhibit the activity of AChE and decrease the absorbance at 412 nm.

## Results and Discussion

#### Inner Filter Effect of AuNPs on the Fluorescence of CdTe QDs

The prepared AuNPs were monitored by the UV–vis absorption spectrum (Fig. 1, curve a), which showed a unique sharp plasmon band at 522 nm, demonstrating that the obtained AuNPs were well dispersed. Water-soluble TGA–CdTe QDs were synthesized via a microwave-assisted heating method. It was difficult to characterize the size of water-soluble CdTe QDs by TEM due to their small dimensions and their tendency to aggregate when drying on a Cu grid (Xue et al. 2011). The absorption spectrum of CdTe QDs (Fig. 1, curve b) indicated that the average particle size of the as-prepared QDs was about 2.3 nm, and the concentration was about  $1.24 \times 10^{-5}$  mol L<sup>-1</sup>, derived from the wavelength of the first excitonic absorption peak at 499 nm based on an empirical fitting function from a previous report (Yu et al. 2003). The obtained CdTe QDs displayed a maximum fluorescence emission at 551 nm (Fig. 1, curve c), which was just near the absorption maximum of AuNPs. It could also be seen that the fluorescence spectrum band was

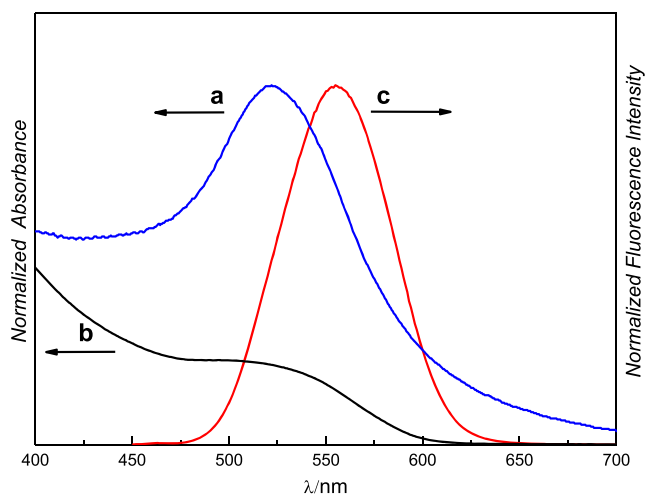


**Fig. 1** Absorption spectra of AuNPs (a) and CdTe QDs (b). The fluorescence emission spectrum of CdTe QDs (c)

relatively narrow and symmetric, which indicated that the obtained CdTe QDs were nearly monodisperse and homogeneous. It was obvious that the absorption spectrum of AuNPs overlaps well with the fluorescence emission spectrum of CdTe QDs. Thus, if the two materials coexist, the effective emission intensity of CdTe QDs might be substantially decreased or even entirely quenched.

As shown in Fig. 2, the emission intensity of CdTe QDs decreased gradually with increasing the concentration of AuNPs. The citrate-stabilized AuNPs in aqueous solution were stabilized against aggregation due to the negative capping agent's (citrate ion) electrostatic repulsion against van der Waals attraction between AuNPs (Grabar et al. 1995; Li et al. 2010). So, AuNPs possessed negative charge, which was further supported by the zeta potential of AuNPs. The dispersed ~13 nm AuNPs displayed the zeta potential of

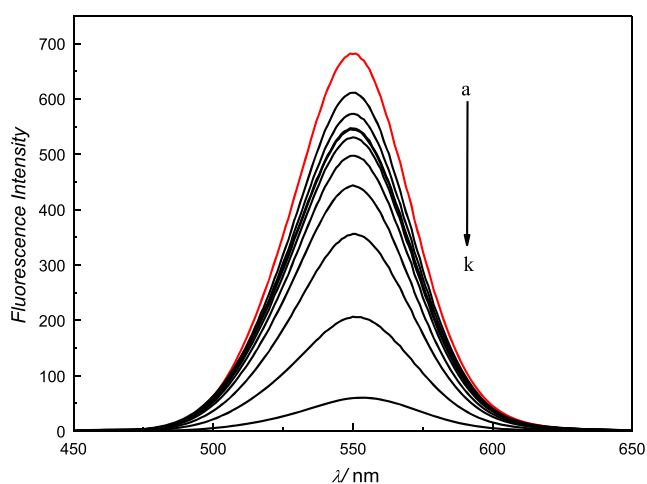


**Fig. 2** Fluorescence emission spectra of CdTe QDs in the presence of increasing concentrations of AuNPs. The concentration of AuNPs in samples (a–k) is 0,  $1.85 \times 10^{-10}$ ,  $3.7 \times 10^{-10}$ ,  $5.55 \times 10^{-10}$ ,  $7.4 \times 10^{-10}$ ,  $9.25 \times 10^{-10}$ ,  $1.11 \times 10^{-9}$ ,  $1.30 \times 10^{-9}$ ,  $1.48 \times 10^{-9}$ ,  $1.67 \times 10^{-9}$ , and  $1.85 \times 10^{-9}$  mol L<sup>-1</sup>, respectively. CdTe QDs,  $1.24 \times 10^{-6}$  mol L<sup>-1</sup>

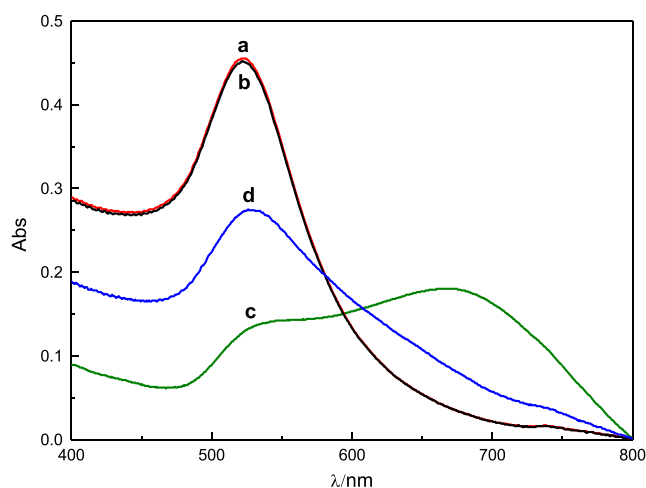
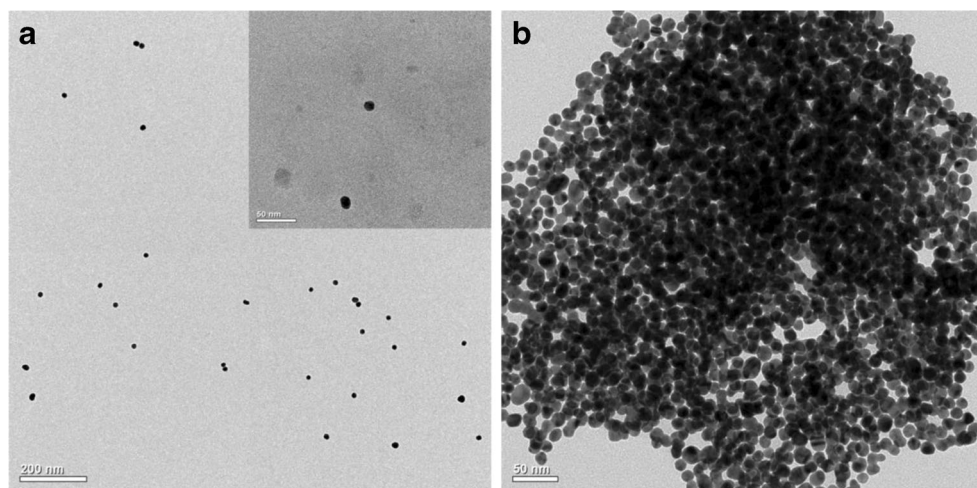


**Fig. 3** Absorption spectra of dispersed AuNPs (a), AuNPs after addition of ATI ( $10 \mu\text{mol L}^{-1}$ ) (b), AuNPs after addition of ATI ( $10 \mu\text{mol L}^{-1}$ ) and AChE ( $1000 \text{ mU mL}^{-1}$ ) (c), and AuNPs after addition of ATI ( $10 \mu\text{mol L}^{-1}$ ), methamidophos ( $0.5 \mu\text{g mL}^{-1}$ ), and AChE ( $1000 \text{ mU mL}^{-1}$ ) (d)

–28.9 mV. The zeta potential of the CdTe QDs was measured to be –20 mV, due to the ionization of the –COOH group in TGA ( $\text{pK}_a=3.53$ ) (Zhang et al. 2003). Thus, there was no electrostatic interaction between AuNPs and CdTe QDs because both of them possessed negative charges. It had been reported that the positively charged QDs could form donor–acceptor assemblies of fluorescence resonance energy transfer (FRET) with negatively charged AuNPs by electrostatic attraction, in which the fluorescence intensity of QDs was effectively quenched, because the electrostatic interaction could shorten the distance between the QDs donor and the AuNPs acceptor (Wang and Ma 2009). It was obvious that an effective FRET donor–acceptor assembly could be hardly established herein due to electrostatic repulsion between the negatively charged AuNPs and the negatively charged CdTe QDs. Fluorescence lifetime, a parameter which was mostly unaffected by IFE, static quenching, and variations in the fluorophore concentration, could provide proof confirming that an efficient FRET process occurs because non-radiative energy transfer was expected to substantially alter the exciton lifetime of the donor. The average lifetime of TGA–CdTe QDs ( $\tau=24.7$  ns) was hardly changed in the presence of AuNPs ( $\tau=24.8$  ns). This result further suggested that the quenched emission of CdTe QDs by AuNPs was not due to the FRET between AuNPs and CdTe QDs. Furthermore, no complex formation or energy transfer was expected between QDs and AuNPs in this system, which was supported by the fact that the Plasmon absorption band of AuNPs remained unchanged in the presence of QDs. Therefore, the observed fluorescence decrease (Fig. 2) should be mainly attributed to the IFE of AuNPs on the fluorescence of CdTe QDs. With increasing the concentration of AuNPs, the absorbance of the absorber increased, which would effectively diminish the emission

**Fig. 4** TEM images of well-dispersed AuNPs (a) and AuNPs after addition of ATI ( $10 \mu\text{mol L}^{-1}$ ) and AChE ( $1,000 \text{ mU mL}^{-1}$ ) (b). The inset in a is TEM image of AuNPs at the scale bar of 50 nm



light from CdTe QDs. As a result, the emission intensity of CdTe QDs gradually decreased. Notably, due to high extinction coefficient of AuNPs, the fluorescence intensity of  $1.24 \times 10^{-6} \text{ mol L}^{-1}$  CdTe QDs decreased by over 90 % in the presence of  $1.85 \times 10^{-9} \text{ mol L}^{-1}$  AuNPs. Therefore, the fluorescence of CdTe QDs at 551 nm can be modulated by the absorbance of AuNPs via IFE in a sensitive and simple approach. Compared to the complicated and costly process to construct QDs–AuNPs FRET assemblies (Oh et al. 2005; Dyadyusha et al. 2005; Tang et al. 2008), this kind of IFE strategy was very practical.

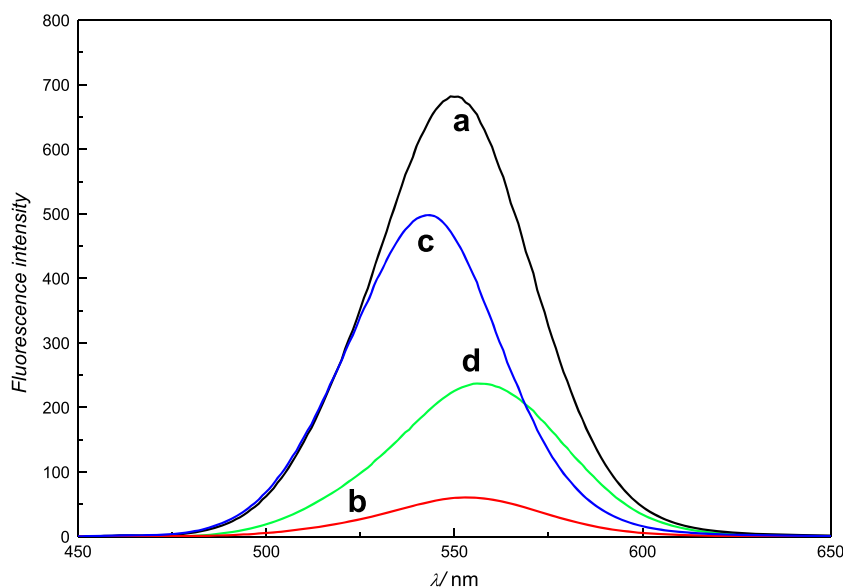
#### Absorbance Changes of AuNPs Caused by the Inhibition of Methamidophos on AChE Activity

As shown in Fig. 3, the addition of ATI ( $10 \mu\text{mol L}^{-1}$ ) almost had no effects on the absorption spectrum of AuNPs (curves a and b). After AChE ( $1000 \text{ mU mL}^{-1}$ ) was further added to the

AuNPs–ATI system and incubated at room temperature for 20 min, the original plasmon absorption of AuNPs at 522 nm decreased with the emergence of a new absorption band at 675 nm (curve c), simultaneously resulting in red-to-purple color changes of AuNPs solution. The spectral changes of curve c in Fig. 3 originated from AChE-catalyzed hydrolysis of ATI into thiocholine, leading to the aggregation of AuNPs. While AChE ( $1,000 \text{ mU mL}^{-1}$ ) was added to the AuNPs–ATI–methamidophos solution, the aggregation of AuNPs and spectral changes could be hindered to some extent due to the inhibition of methamidophos on AChE activity (curve d).

The aggregation of AuNPs induced by the AChE-catalyzed hydrolysis of ATI was further confirmed by the TEM images (Fig. 4). The as-prepared AuNPs were well dispersed with uniform particle size (Fig. 4a). The scale bar of the inset in Fig. 4a was 50 nm, which indicated that the particle diameter of AuNPs was about 13 nm. However, after addition of ATI and AChE, the AuNPs aggregated together (Fig. 4b). The

**Fig. 5** Fluorescence emission spectra: a CdTe QDs; b CdTe QDs and AuNPs; c mixture of AuNPs, ATI, AChE, and CdTe QDs; d mixture of AuNPs, ATI, AChE, methamidophos, and CdTe QDs. CdTe QDs,  $1.24 \times 10^{-6} \text{ mol L}^{-1}$ ; AuNPs,  $1.85 \times 10^{-9} \text{ mol L}^{-1}$ ; ATI,  $10 \mu\text{mol L}^{-1}$ ; AChE,  $1,000 \text{ mU mL}^{-1}$ ; methamidophos,  $2 \mu\text{g mL}^{-1}$



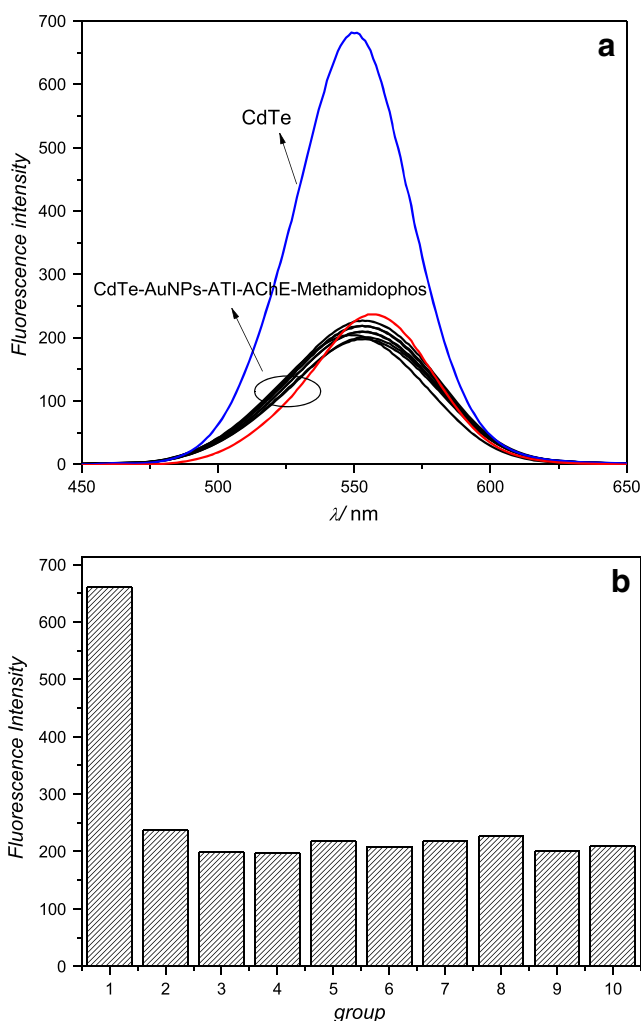


**Fig. 6** Fluorescence spectra (a) and the corresponding fluorescence intensity (b) of CdTe–AuNPs–ATI–AChE in the presence of 2 μg mL<sup>-1</sup> methamidophos premixed with different substances. The red line is the fluorescence spectrum of CdTe–AuNPs–ATI–AChE–methamidophos. Substances: 1 CdTe, 2 control (CdTe–AuNPs–ATI–AChE–methamidophos), 3 vitamin C (0.16 mg mL<sup>-1</sup>), 4 vitamin B<sub>1</sub> (0.007 mg mL<sup>-1</sup>), 5 vitamin B<sub>2</sub> (0.0013 mg mL<sup>-1</sup>), 6 Fe<sup>3+</sup> (0.019 mg mL<sup>-1</sup>), 7 Na<sup>+</sup> (0.430 mg mL<sup>-1</sup>), 8 Mg<sup>2+</sup> (0.43 mg mL<sup>-1</sup>), 9 Zn<sup>2+</sup> (0.015 mg mL<sup>-1</sup>), 10 K<sup>+</sup> (0.29 mg mL<sup>-1</sup>)

results of TEM analysis were consistent with the UV–vis absorption spectra and confirmed directly the experimental observations discussed above. Thus, AChE-catalyzed hydrolysis of acetylthiocholine into thiocholine could lead to the absorption changes of AuNPs, which would be hindered by OPs due to their inhibition on AChE activity.

#### Fluorescence Detection of Methamidophos Through the IFE of AuNPs on the Fluorescence of CdTe QDs

As was mentioned above, AChE-catalyzed hydrolysis of acetylthiocholine into thiocholine could lead to the aggregation of AuNPs with spectral and color changes, which

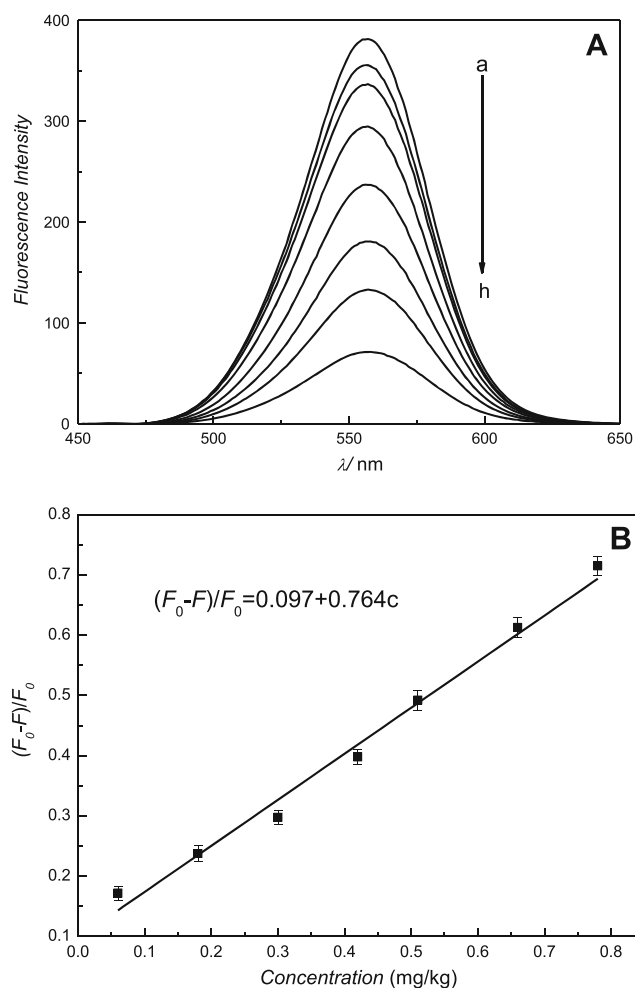


**Fig. 7** a Fluorescence emission spectra of CdTe–AuNPs–ATI–AChE system in the presence of increasing concentrations of methamidophos spiked in Chinese cabbage (a–h, respectively, with the concentration of 0, 0.06, 0.18, 0.3, 0.42, 0.54, 0.66, and 0.78 mg/kg). b The linear calibration of (F<sub>0</sub>-F)/F<sub>0</sub> versus methamidophos concentration spiked in Chinese cabbage

could be hindered by OPs due to their inhibition on AChE activity, while the fluorescence emission of CdTe QDs could be effectively quenched by the IFE of AuNPs. It was reasonable to expect that the IFE efficiency of AuNPs on CdTe QDs would be affected by the hydrolysis reaction of AChE–acetylthiocholine and the presence of OPs. Thus, the IFE-based ODs emission would respond to OPs concentration under certain experimental conditions (Scheme 1). As shown in Fig. 5, the fluorescence of CdTe QDs (curve a) was obviously quenched in the presence of AuNPs via IFE (curve b). After AChE (1,000 mU mL<sup>-1</sup>) was further added to the CdTe–AuNPs–ATI system, the IFE-decreased fluorescence of QDs was recovered obviously (curve c) because AChE-catalyzed hydrolysis of acetylthiocholine induced the aggregation and absorbance decrease of AuNPs. Additionally, the presence of OPs could irreversibly inhibit the catalytic activity of AChE and the aggregation of AuNPs, and the

**Table 1** Application of the proposed method for determination of methamidophos in Chinese cabbage spiked with different amounts of methamidophos

Sample	Amount added (mg/kg)	Amount found (mg/kg)	Recovery±RSD % ( <i>n</i> =3)
Chinese cabbage	0.06	0.067	112.1±1.8
	0.30	0.293	97.8±1.7
	0.60	0.574	95.7±2.8

emission spectra were decreased again at a certain degree (curve d). Thus, the fluorescence emission of CdTe QDs could be modulated by the absorption of AuNPs which varied with the concentration of OPs, making the fluorescence analysis of pesticides feasible.

#### IFE-Based Fluorescent Sensing of Methamidophos in Spiked and Real Vegetable Samples

Interference studies were done in order to explore the specific detection of methamidophos in vegetables using the proposed assay. These experiments included investigation of most commonly found substances in real samples of vegetables, such as vitamin C, vitamin B<sub>1</sub>, vitamin B<sub>2</sub>, Fe<sup>3+</sup>, Na<sup>+</sup>, Mg<sup>2+</sup>, Zn<sup>2+</sup>, and K<sup>+</sup>. As shown in Fig. 6, no obvious interferences were noticed with the presence of these selected ions and compounds for determination of methamidophos (i.e., the relative error in all the cases was less than 10 %). Therefore, the results showed no interferences from these substances in concentration levels usually found in vegetable samples.

To validate the proposed method to specifically detect methamidophos in vegetables, different amounts of methamidophos were added into Chinese cabbage. Then, the spiked samples were pretreated and analyzed according to the procedure described in “Procedures for Methamidophos Sensing in Spiked and Real Vegetable Samples.” Figure 7a showed the fluorescence spectral changes of the solutions in the absence and presence of different concentrations of methamidophos. And the  $(F_0 - F)/F_0$  was related linearly to the concentration of methamidophos spiked in Chinese cabbage in the range of 0.06–0.78 mg/kg as displayed in Fig. 7b. The detection limit was calculated as 2 μg/kg following the IUPAC criteria, defined by  $3S_0/K$  where  $S_0$  is

the standard deviation of blank measurements (*n*=7) and *K* is the slope of calibration graph. The relative standard deviation (RSD) was 4.3 % for the determination of 0.3 mg/kg methamidophos (*n*=7), implying good reproducibility of the proposed assay. The proposed method was applied to analyze methamidophos in the spiked samples of Chinese cabbage, and the recovery results were listed in Table 1, which indicated that the proposed IFE-based fluorescence sensing was highly reproducible and accurate for the analysis of methamidophos in vegetable in a simple manner. In addition, the obtained detection limit is below the maximum residue limit of methamidophos established by Chinese regulation (0.05 mg/kg, Chinese National Standards (2012) GB 2763-2012), so this method has promising application in the rapid screening of methamidophos.

It is worth noting that even though the same experimental procedures are used for nanomaterial synthesis, especially for QDs, many experimental variables would mean that each batch of AuNPs/QDs might have slightly different absorption/emission profiles. Thus, it is essential to establish the calibration curve for each batch of AuNPs/QDs.

We used the IFE-based fluorescence sensing and the enzyme inhibition rate method of GB/T 5009.199-2003 to determine the content of methamidophos in Chinese cabbage. The obtained results demonstrate that organic vegetables which were used as samples have no methamidophos contamination. In order to explore the application of the proposed fluorescent biosensor for OPs analysis in real sample, the samples of Chinese cabbage free from OPs were immersed in 1 μg mL<sup>-1</sup> methamidophos for 24 h and then rinsed several times with distilled water. After that, the obtained samples were pretreated and analyzed according to the procedure described in “Procedures for Methamidophos Sensing in Spiked and Real Vegetable Samples,” at the same time, detected following the method of GB/T 5009.199-2003. As shown in Table 2, the obtained methamidophos content of the contaminated vegetables from the two methods was in good accordance. The slight difference might be attributed to the different conditions and assay procedures. In addition, the proposed fluorescent assay had a lower detection limit and much higher sensitivity. Thus, the proposed method was credible for methamidophos detection and could be applied to rapid screening of methamidophos in real samples.

**Table 2** Comparison of analytical results between the proposed method and GB/T 5009.199-2003 method

Method	The purposed method	GB/T 5009.199-2003
Linear range (mg/kg)	0.06~0.78	0.14~4.20
Linear regression equation	$(F_0 - F)/F_0 = 0.097 + 0.764c$	Inhibition% = $0.50c + 0.09$
Linear correlation coefficient ( <i>r</i> )	0.9939	0.9868
Detection limit (mg/kg)	0.002	0.05
Measured value (mg/kg)	0.246 (RSD = 1.3 %, <i>n</i> =3)	0.237 (RSD = 2.7 %, <i>n</i> =3)



Similar to other biosensors including GB/T 5009.199-2003, which are based on the enzyme inhibition action of OPs on cholinesterases, the proposed IFE assay supplies the total amount of OPs in samples, and at this stage, is not capable to distinguish the different kinds of OPs. Therefore, the simultaneous presence of various OPs in contaminated samples provides a challenge for the application for purely regulatory purposes where a specific analyte must be determined with a prescribed accuracy. Nevertheless, many advantages provided by the established sensor, such as easy sample pretreatment, rapid and high sensitivity, and low cost, could facilitate future development of rapid, high-throughput screening of OPs residues. This novel nano-biosensor might be used as an alarm system on-line and on site, which would provide either quantification of one contaminant when this analyte is present alone or an indication of total contamination of particular samples.

## Conclusions

In this study, a novel sensitive and rapid fluorescent assay based on the inner filter effect (IFE) of AuNPs on CdTe QDs for detection of organophosphorus pesticides (OPs) residues was developed. The IFE efficiency of AuNPs on CdTe QDs varied with the absorption of AuNPs. AChE-catalyzed hydrolysis of acetylthiocholine into thiocholine could lead to the aggregation of AuNPs accompanied by the decrease of their surface plasmon absorption, which could be hindered by OPs due to their inhibition on AChE activity. The present IFE-based assay allowed the design of fluorescent methods in a more rapid and simple way. Taking methamidophos as the representative pesticide, the fluorescent detection of OPs in vegetables using QDs as probe has been achieved with satisfactory results. This detection method showed high precision and sensitivity, with a detection limit as low as 2 µg/kg, which was much lower than the detection limit of GB/T 5009.199-2003 method. Therefore, the proposed rapid assay provides a new promising tool for the OPs screening.

**Acknowledgments** This work was financially supported by the Natural Science Foundation of Jilin Province (no. 201215024) and Innovation Projects of Science Frontiers and Interdisciplinary of Jilin University.

**Conflict of Interest** Jiajia Guo declares that she has no conflict of interest. Yeli Luo declares that she has no conflict of interest. Hongkun Li declares that she has no conflict of interest. Minwei Zhang declares that he has no conflict of interest. Xianyi Cao declares that he has no conflict of interest. Fei Shen declares that she has no conflict of interest. Chunyan Sun declares that she has no conflict of interest. Jingbo Liu declares that she has no conflict of interest. This article does not contain any studies with human or animal subjects.

## References

- Byers RJ, Hitchman ER (2011) *Prog Histochem Cytochem* 45:201–237
- Chai MK, Tan GH (2009) *Food Chem* 117:561–567
- Chauhan N, Pundir CS (2012) *Electrochim Acta* 67:79–86
- Chinese National Standards (2012) GB 2763-2012. National food safety standard Maximum residue limits for pesticides in food. Standards Press of China, Beijing
- Chinese National Standards (2003) GB/T5009.199-2003. Rapid determination for organophosphate and carbamate pesticide residues in vegetables. Standards Press of China, Beijing
- Dyadyusha L, Yin H, Jaiswal S, Brown T, Baumberg JJ, Booy FP, Melvin T (2005) *Chem Commun* 25:3201–3203
- Frasco MF, Chaniotakis N (2009) *Sensors* 9:7266–7286
- Gill R, Zayats M, Willner I (2008) *Angew Chem* 47:602–625
- Grabar KC, Freeman RG, Hommer MB, Natan MJ (1995) *Anal Chem* 67:735–743
- Li HK, Guo JJ, Ping H, Liu LR, Zhang MW (2011) Guan FR. Sun CY, Zhang Q
- Li L, Li BX, Cheng D, Mao LH (2010) *Food Chem* 122:895–900
- Liu DB, Chen WW, Wei JH, Li XB, Wang Z, Jiang XY (2012) *Anal Chem* 84:4185–4191
- Liu SQ, Yuan L, Yue XL, Zheng ZZ, Tang ZY (2008) *Adv Powder Technol* 19:419–441
- Meng XW, Wei JF, Ren XL, Ren J, Tang FQ (2013) *Biosens Bioelectron* 47:402–407
- Oh E, Hong MY, Lee D, Nam SH, Yoon HC, Kim HS (2005) *J Am Chem Soc* 127:3270–3271
- Perez-Ruiz T, Martínez-Lozano C, Tomás V (2005) *Anal Chim Acta* 540: 383–391
- Pérez-Ruiz T, Martínez-Lozano C, Tomás V, Martín J (2001) *Talanta* 54: 989–995
- Periasamy AP, Umasankar Y, Chen SM (2009) *Sensors* 9:4034–4055
- Qu LJ, Zhang H, Zhu JH, Yang GS, Aboul-Enein HY (2010) *Food Chem* 122:327–332
- Shang L, Dong SJ (2009) *Anal Chem* 81:1465–1470
- Sanz CP, Halko R, Ferrera ZS (2004) *Anal Chim Acta* 524:265–270
- Shao N, Zhang Y, Cheung SM, Yang RH, Chan WH, Mo T, Li KA, Liu F (2005) *Anal Chem* 77:7294–7303
- Tang B, Cao LH, Xu KH, Zhuo LH, Ge JC, Li QL, Yu LJ (2008) *Chem-A Eur J* 14:3637–3644
- Wang X, Guo XQ (2009) *Analyst* 134:1348–1354
- Wang YX, Xiong LM, Geng FH, Zhang FQ, Xu MT (2011) *Analyst* 136: 4809–4814
- Wang ZX, Ma LN (2009) *Coord Chem Rev* 253:1607–1618
- Xu L, Li BX, Jin Y (2011) *Talanta* 84:558–564
- Xue M, Wang X, Wang H, Chen DZ, Tang B (2011) *Chem Commun* 47: 4986–4988
- Xue R, Kang TF, Lu LP, Cheng SY (2012) *Appl Surf Sci* 258: 6040–6045
- Yu WW, Qu LH, Guo WZ, Peng XG (2003) *Chem Mater* 15:2854–2860
- Yu T, Shen JS, Bai HH, Guo L, Tang JJ, Jiang YB, Xie JW (2009) *Analyst* 134:2153–2157
- Yuan P, Walt DR (1987) *Anal Chem* 59:2391–2394
- Zhang MW, Ping H, Cao XY, Li HK, Guan FR, Sun CY, Liu JB (2012) *Food Addit Contam* 29:333–344
- Zhang H, Zhou Z, Yang B (2003) *J Phys Chem B* 107:8–13
- Zhao WA, Brook MA, Li YF (2008) *ChemBioChem* 9:2363–2371
- Zheng ZZ, Zhou YL, Li XY, Liu SQ, Tang ZY (2011) *Biosens Bioelectron* 26:3081–3085